Long-Period Equatorial Topographic Waves[1]

LAWRENCE A. MYSAK[2]

National Center for Atmospheric Research,[3] Boulder, Colo. 80307

(Manuscript received 1 August 1977, in final form 21 November 1977)

ABSTRACT

A theory of barotropic, nondivergent, zonally propagating waves on an equatorial beta-plane with topography is presented. The bottom contours are assumed to be parallel to the equator, so that the depth profile H is a function only of y, the northward coordinate. Solutions for trapped waves are derived for the following depth profiles: 1) a single-step escarpment, 2) a flat continental shelf, 3) a semi-infinite sloping beach, and 4) an exponentially varying continental shelf/slope region that monotonically increases to a constant depth far from the shoreline. For each wave solution presented, numerical examples of typical periods and phase speeds are also given. The eigenfrequencies ω_n for the waves trapped on a sloping beach with depth profile $H = H_0 + \alpha y$ take a particularly simple form: $\omega_n = -\beta H_0/|\alpha|(2n + 3)$, where $n = 0, 1, 2, \ldots$, and $\beta = 2\Omega_E/R$ (Ω_E and R are the earth's angular speed of rotation and radius, respectively). A number of qualitative results are also derived. For example, a WKB-type argument is used to show that equatorial trapping will always occur over any monotonic depth profile that straddles the equator. Also, it is proved that the phase of an equatorial topographic wave propagates westward or eastward according to whether the equilibrium potential vorticity $\beta y/H(y)$ is a monotonic increasing or decreasing function of y.

1. Introduction

In the last two decades increasing attention has been devoted to the study of large-scale tropical ocean currents. In attempts to understand the dynamics of these currents, which are primarily driven by the trade winds, investigators have developed essentially two types of models: 1) linear, initial-value, wave-type models and 2) linear and nonlinear, steady-state circulation models [see Moore and Philander (1977) for a recent overview]. In the first group of models it is shown how the currents can be generated by the sudden application of a prescribed wind-stress field to an initially calm, stably stratified inviscid ocean. The response in these models is represented by a superposition of the equatorial wave modes that can exist in an equatorial β-plane ocean of uniform depth. In the second group of models, steady-state, wind-driven circulation patterns are studied on the assumption that these patterns may eventually result from the transient, wave-like motions found in the first group of models. The more recent modeling efforts, however, have attempted to join these two types of responses. For example, Anderson and Rowlands (1976) and Cox (1976) have studied the evolution of an initially generated equatorial wave pattern in the Indian Ocean into a steady coastal current that models the Somali Current off the east coast of Africa.

In the theoretical studies described above, it is assumed that the effects of topography are negligible. However, a glance at a bathymetric chart of the tropical oceans reveals the presence of trenches, mountain ridges, escarpments and continental shelf/slope regions that either cut across or run nearly parallel to the equator. Thus it is natural to ask what effects these topographic features have on equatorial waves and hence how topography affects the results found in the earlier studies on tropical currents. Since long-period waves at mid-latitudes can be strongly affected and even dominated by large-scale topographic features (Rhines, 1977; LeBlond and Mysak, 1977, 1978), it is conceivable that topography may play an important role in equatorial wave propagation. Moreover, as Moore and Philander (1977) pointed out, before the actual bathymetry of the ocean floor is incorporated into sophisticated numerical models of the tropical oceans, it is valuable to know, in idealized situations, how topography influences equatorial waves. Indeed, in recent numerical experiments designed to study wave propagation around the North Atlantic basin it was found that the incorporation of the ba-

[1] Dedicated to Professor George F. Carrier on the occasion of his sixtieth birthday.

[2] Permanent affiliation: Department of Mathematics and Institute of Oceanography, University of British Columbia, Vancouver, B.C. Canada V6T 1W5.

[3] The National Center for Atmospheric Research is sponsored by the National Science Foundation.

0022-3670/78/0302-0314$06.50

thymetry completely altered the picture. With topography included, an elementary description in terms of equatorial and coastal waves was no longer possible (D. Anderson, 1977, personal communication).

In this paper we investigate the properties of zonally propagating, long-period equatorial waves in a simple tropical ocean model with topography. We assume that the motions are barotropic and nondivergent, and that the isobaths are parallel to the equator. The governing equations for this model are presented in Section 2, along with the appropriate boundary and matching conditions. The solutions for waves trapped along a single-step escarpment and a flat continental shelf are given in Sections 3 and 4, respectively. These waves are the equatorial counterparts of the mid-latitude double Kelvin wave and the continental shelf wave which were first studied in terms of these topographic models by Rhines (1967, 1969) and Larsen (1969), respectively. The solution for a trapped wave on a sloping beach is given in Section 5. Its mid-latitude kin is the trapped quasi-geostrophic wave on a sloping beach investigated by Reid (1958). In Section 6 the solution for trapped waves on an exponential depth profile is presented. This profile, first introduced by Ball (1967) in a study of edge waves at mid-latitudes, reduces to a uniformly sloping beach region close to shore and asymptotes smoothly to a constant depth region far from shore. Finally, in Section 7 some qualitative results concerning trapped waves over arbitrary profiles are established.

2. Governing equations

The linearized equations for barotropic, nondivergent motions on an equatorial β-plane with depth profile $H(y)$ are given by

$$\left.\begin{aligned} u_t - \beta y v + \rho^{-1} p_x &= 0 \\ v_t + \beta y u + \rho^{-1} p_y &= 0 \end{aligned}\right\}, \tag{2.1}$$

$$H u_x + (Hv)_y = 0, \tag{2.2}$$

where u, v are the velocity components in the x (eastward), y (northward) directions, p is the pressure, ρ the density and $\beta = 2\Omega_E/R$, Ω_E and R being the earth's angular speed of rotation and radius, respectively. In view of (2.2) we can express the velocity components in terms of a mass transport streamfunction $\Psi(x,y,t)$:

$$u = -\Psi_y/H, \quad v = \Psi_x/H. \tag{2.3}$$

Substituting (2.3) into (2.1) and then eliminating p, we obtain the vorticity balance equation

$$H^{-1}\Psi_{txx} + (H^{-1}\Psi_{ty})_y + \beta(H^{-1}y)_y\Psi_x = 0. \tag{2.4}$$

For zonally propagating waves of the form

$$\Psi = \psi(y)e^{i(kx-\omega t)}, \quad k > 0, \tag{2.5}$$

(2.4) reduces to

$$(H^{-1}\psi')' - [H^{-1}k^2 + (k\beta/\omega)(H^{-1}y)']\psi = 0, \tag{2.6}$$

where the prime indicates d/dy. To complement (2.6) we need to impose certain boundary and matching conditions.

If there are no boundaries to the north and to the south, we shall require that

$$\psi \to 0 \quad \text{as} \quad y \to \pm\infty, \tag{2.7a}$$

i.e., the waves are trapped near the equator. On the other hand, if the ocean is of semi-infinite extent, with $y_c \leqslant y \leqslant \infty$, say, we shall require that

$$\psi \to 0 \quad \text{as} \quad y \to +\infty \tag{2.7b}$$

and

$$\psi = 0 \quad \text{at} \quad y = y_c. \tag{2.8}$$

The last condition applies when 1) there is a vertical wall at $y = y_c$ or 2) the depth goes to zero at $y = y_c$ (a shoreline). If there is a discontinuity in the depth at $y = y_e$, say, we require that the normal transport Hv be continuous at $y = y_e$. From (2.3) and (2.5) we thus obtain the jump condition

$$[\psi] = 0 \quad \text{at} \quad y = y_e. \tag{2.9}$$

A second jump condition is obtained by integrating (2.6) over the interval $(y_e - \epsilon, y_e + \epsilon)$ and then taking the limit $\epsilon \to 0$. The result is

$$[H^{-1}\psi'] - (\beta k y_e/\omega)\psi(y_e)[H^{-1}] = 0 \quad \text{at} \quad y = y_e, \tag{2.10}$$

where (2.9) has been used. Physically, (2.10) guarantees that the pressure is continuous at $y = y_e$. We note that since $H^{-1}\psi' \propto u$, Eq. (2.10) implies that there is a vortex sheet at $y = y_e$, unless, of course, $y_e = 0$.

3. The equatorial double Kelvin wave

As our first example we discuss the trapping of a wave along the single-step escarpment

$$H(y) = \begin{cases} H_1, & y_e < y \leqslant \infty \\ H_2, & -\infty \leqslant y < y_e. \end{cases} \tag{3.1}$$

Rhines (1967, 1969) was the first to use this form for $H(y)$ to study the topographic trapping of long-period waves at mid-latitudes. Substituting (3.1) into (2.6) we find that on either side of the escarpment, the amplitude $\psi(y)$ satisfies the equation

$$\psi'' - (k^2 + k\beta/\omega)\psi = 0. \tag{3.2}$$

The solution of (3.2) which satisfies the trapping condition (2.7a) and the jump condition (2.9) is given by

$$\psi = Ae^{-K|y-y_e|}, \tag{3.3}$$

where A is an arbitrary constant and $K = (k^2 + k\beta/\omega)^{1/2} > 0$. Because (3.3) decays exponentially for both $y > y_e$ and $y < y_e$, Longuet-Higgins (1968) called a solution of the form (3.3) a "double Kelvin wave". The dispersion relation is determined by requiring (3.3) to satisfy the second jump condition (2.10). The result is

$$\omega K = \beta k y_e \frac{1-\delta}{1+\delta}, \tag{3.4}$$

where $\delta = H_2/H_1$. Eq. (3.4) is the analog of the dispersion relation obtained by Rhines (1967, 1969) for a long-period wave trapped on a mid-latitude escarpment on an f-plane, *viz.*,

$$\omega = f\frac{1-\delta}{1+\delta}, \tag{3.4}'$$

where f is the (constant) Coriolis parameter. Note that the above relation implies that the group velocity $\partial\omega/\partial k$ is zero for all k. On the other hand, (3.4) implies that $\partial\omega/\partial k \neq 0$ for the equatorial double Kelvin wave.

We first note that (3.4) is invariant under the transformation

$$\delta \to 1/\delta, \quad y_e \to -y_e. \tag{3.5}$$

Therefore, without loss of generality, we need only consider the case $\delta < 1$, with $y_e > 0$ or $y_e < 0$. When $y_e > 0$ (depth discontinuity in Northern Hemisphere), Eq. (3.4) implies that $\omega > 0$ since $K > 0$, $k > 0$ and $\beta > 0$. This means that the wave phase propagates eastward with the shallow water to the right. When $y_e < 0$ (depth discontinuity in Southern Hemisphere), on the other hand, the phase propagates westward with the shallow water to the left. Thus we conclude that the usual rule for the direction of phase propagation of topographic Rossby waves on an f-plane at mid-latitudes also carries over to the zonally propagating equatorial double Kelvin wave. It is interesting to note that if $y_e = 0$, Eq. (3.4) implies that the only wave solution is $K = 0$ (no trapping possible) and hence, from the definition of K, $\omega = -\beta/k$, the usual dispersion relation for a one-dimensional, westward-propagating Rossby wave.

If we square (3.4) and solve the resulting quadratic for ω, we obtain

$$\Omega \equiv \frac{\omega}{\beta|y_e|} = (1/2\kappa)[-1 + \mathrm{sgn}\, y_e(1 + 4\Delta^2\kappa^2)^{1/2}],$$

where $\kappa = k|y_e|$ and $\Delta^2 = (1-\delta)^2/(1+\delta)^2$. This relation is plotted in Fig. 1 for the case $\delta = \frac{1}{2}$. From this figure we note that while the phase propagation changes direction according to the location of the depth discontinuity, the energy always propagates eastward. A similar result was also obtained by Rhines (1969) when the β-effect was incorporated into his mid-latitude double Kelvin wave solution. In fact our Fig. 1 is analogous to the case $\alpha = 0$ in Fig. 10 of Rhines (1969).

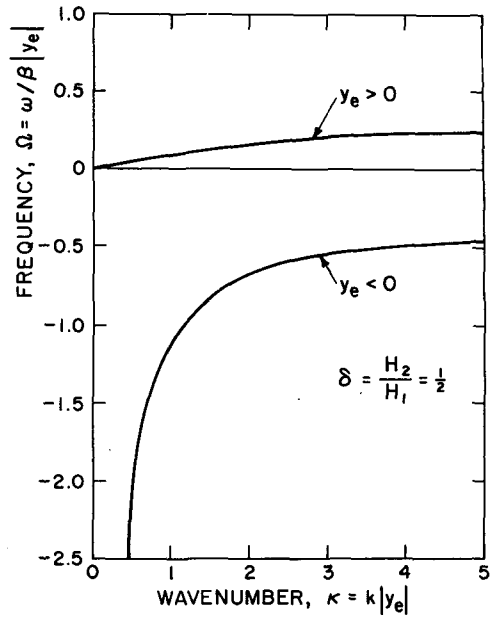

FIG. 1. The dispersion relation (3.6) for an equatorial double Kelvin wave traveling along the discontinuous depth profile (3.1). Since the dispersion relation is invariant under the transformation (3.5), the upper (lower) curve also applies to the case $\delta = 2$ and $y_e < 0$ ($y_e > 0$).

A few numerical examples of the period and phase speed of an equatorial double Kelvin wave are given in Table 1 for the case in which the depth discontinuity is located either 500 km north or 500 km south of the equator. Note that the westward propagating waves ($y_e < 0$) travel considerably faster than the corresponding eastward propagating waves ($y_e > 0$). This large numerical asymmetry in the phase speed is completely absent for double Kelvin waves on a mid-latitude escarpment: Eq. (3.4)′ implies that the phase speed in the Southern Hemisphere is just the negative of that in the northern hemisphere.

TABLE 1. The period and phase speed of an equatorial double Kelvin for two prescribed wavelengths. In all cases $\delta = H_2/H_1 = 0.5$ as in Fig. 1.

Wavelength (km)	Period (days)		Phase speed (km day^{-1})	
	y_e = 500 km,	y_e = −500 km	y_e = 500 km,	y_e = −500 km
1000	30.3	11.8	33.0	84.8
3000	63.7	6.07	47.1	494

If the depth profile across the escarpment region is continuous rather than discontinuous, then the escarpment behaves like a potential well, with the amplitude $\psi(y)$ being oscillatory over the escarpment and decaying on either side of it. Further, in this case there exists an infinity of escarpment modes, of which the fundamental one reduces to (3.3) as the escarpment width tends to zero. An example of such modal solutions for the case of mid-latitude double Kelvin waves on the f-plane is given in Rhines (1969). Another possibile extension of the theory presented here is to include the free-surface divergence, which will likely be important at long wavelengths. For the mid-latitude case this extension has been carried out by Longuet-Higgins (1968).

4. Equatorial shelf waves on a flat shelf

We now investigate the propagation of a continental shelf wave trapped along a flat shelf. The depth profile is a slight variant of (3.1):

$$H(y) = \begin{cases} H_1, & y_e < y \leq \infty \\ H_2, & y_c \equiv y_e - l \leq y < y_e \end{cases} \tag{4.1}$$

where $H_1 > H_2$ (deep water to the north) and l is the shelf width. The case of a shelf with deep water to the south will be discussed later. The equation for the amplitude $\psi(y)$ in both the shelf ($y_c \leq y < y_e$) and deep sea regions ($y_e < y \leq \infty$) regions again takes the form (3.2). The solution for ψ which satisfies (3.2) in each region, the boundary conditions (2.7b) and (2.8), and the jump condition (2.9) is given by

$$\psi = \begin{cases} A \sinh K(y - y_e + l), & y_e - l \leq y < y_e \\ A \sinh Kl e^{-K(y-y_e)}, & y_e < y \leq \infty \end{cases} \tag{4.2}$$

The substitution of (4.2) into the jump condition (2.10) gives

$$\omega K(\delta \sinh Kl + \cosh Kl) = \beta k y_e (1 - \delta) \sinh Kl \tag{4.3}$$

for the dispersion relation. As in Section 3, $\delta = H_2/H_1$, and $\delta < 1$ for deep water to the north. We also note that in the wide-shelf limit $Kl \to \infty$, (4.3) reduces to (3.4), the dispersion relation for a single-step escarpment.

The solution (4.2), (4.3) is the equatorial counterpart to the "quasi-geostrophic" wave solution found by Larsen (1969) [see also LeBlond and Mysak (1977) for an elementary account of this solution]. To obtain Larsen's mid-latitude solution from (4.3), replace K by k and βy_e by f, the Coriolis parameter, which yields an explicit relation for ω as a function of k. By way of contrast, (4.3) is an implicit relation between ω and k. Therefore, to solve for ω as a function of k one must use an iterative numerical scheme. Nevertheless, certain qualitative results about the direction of phase propagation can be determined directly from (4.3), without recourse to numerical computations. Before discussing these results, however, we now give the solution for a shelf with deep water to the south.

For the depth profile

$$H(y) = \begin{cases} H_1, & y_e < y \leq y_c \equiv y_e + l \\ H_2, & -\infty \leq y < y_e \end{cases} \tag{4.4}$$

where $H_1 < H_2$, ψ takes the form

$$\psi = \begin{cases} A \sinh K(y - y_e - l), & y_e < y \leq y_e + l \\ -A \sinh Kl e^{K(y-y_e)}, & -\infty \leq y < y_e. \end{cases} \tag{4.5}$$

The dispersion relation corresponding to (4.5) is given by

$$\omega K(\delta \cosh Kl + \sinh Kl) = \beta k y_e (1 - \delta) \sinh Kl, \tag{4.6}$$

which also reduces to (3.4) in the limit $Kl \to \infty$.

Although (4.6) is not identical to (4.3), the transformation (3.5) takes (4.6) into that form. Therefore, we again need only focus our attention on (4.3). Since $\delta < 1$ for the shelf model (4.1) and K, l, k and β are all positive, it again follows from (4.3) that the shallow water is to the right (left) of the direction of phase propagation when the depth change is in the Northern (Southern) Hemisphere. [It is also interesting to note that if $\delta > 1$ (a deep trench against the coast), (4.3) implies that the same principle holds, although in this case the shallow water is of semi-infinite extent.]

In terms of the nondimensional frequency $\Omega = \omega/\beta|y_e|$ and wavenumber $\kappa = k|y_e|$, the dispersion relation (4.3) can be written as

$$\Omega = \frac{\operatorname{sgn} y_e \kappa (1 - \delta) \sinh \chi r}{\chi(\delta \sinh \chi r + \cosh \chi r)}, \tag{4.7}$$

where $\chi = (\kappa^2 + \kappa/\Omega)^{1/2}$ and $r = l/|y_e|$. The curves Ω vs κ for various values of r and δ are shown in Figs. 2 and 3.

From Fig. 2, the case $y_e > 0$, we note that the phase and group velocities are always directed eastward. For fixed r (shelf width), the phase speed increases inversely with δ, that is, as H_2/H_1 decreases. Also, we note that for fixed δ the phase speed increases with r (shelf width), although for $r > 1$ the changes in the phase speed are very small. Indeed, the $\delta = 0.5$ curve in Fig. 2c is almost identical to the upper curve in Fig. 1 (the case $r = \infty$). The qualitative properties of the dispersion relations shown in Fig. 2 are very similar to those for a mid-latitude flat shelf. Finally, we remark that in view of the relationship between (4.3) and (4.6), any curve labeled δ_0 in Fig. 2 also applies to the case

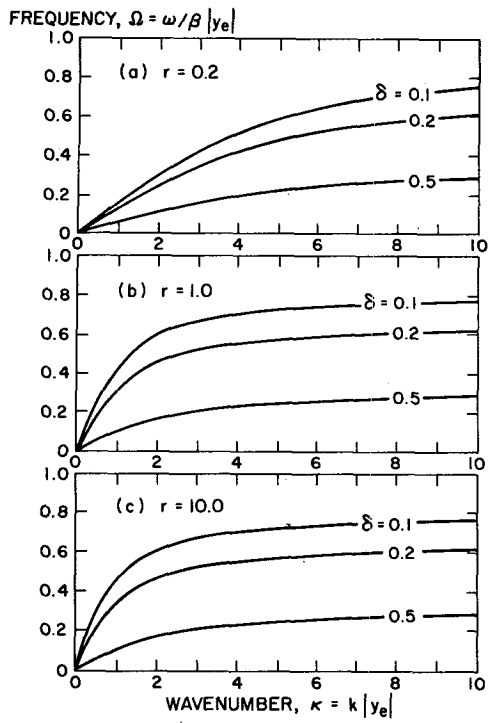

FIG. 2. The dispersion relation (4.7) for $y_e > 0$. The parameter $r = l/|y_e|$ is a measure of the shelf width. The parameter $\delta = H_2/H_1$ is the ratio of the shelf depth to deep-sea depth.

$y_e < 0$ and $\delta_1 = 1/\delta_0$ (shelf break in Southern Hemisphere and deep water to the south).

From Fig. 3, the case $y_e < 0$, we see that there is a long-wave cutoff for the existence of a trapped wave, a result which is unique to the equatorial flat shelf. To the left of each curve, $K^2 + K/\Omega < 0$ and hence the exponential term in (4.2) becomes oscillatory, the result being that energy radiates away from the shelf in the form of a Rossby wave. This behavior can be explained physically if we recall that the Fig. 3 curves correspond to the case where the shelf is in the Southern Hemisphere whereas the bulk of the deep sea region is in the Northern Hemisphere. Thus there is a delicate balance between the restoring force due to topography (which tends to send the wave directly westward) and that due to planetary vorticity (which tends to send the wave northwestward). For large-scale motions (small κ), the β-effect dominates and the waves cannot be trapped against the shell. Another interesting feature evident from Fig. 3 is the existence of a zero group velocity at intermediate wavenumbers for the cases $r = 0.5, 1$. That is, the direction of energy propagation changes sign, being along the phase velocity at long wavelengths and opposite to the phase velocity at short wavelengths. The same phenomenon occurs for shelf waves at mid-latitudes over a certain type of exponential shelf profile on the f-plane (see LeBlond and Mysak, 1977, Fig. 14). For small (large) r, however, the group velocity is always westward (eastward) and hence is in (against) the direction of the phase velocity. Finally, we remark any curve labeled δ_0 in Fig. 3 also applies to

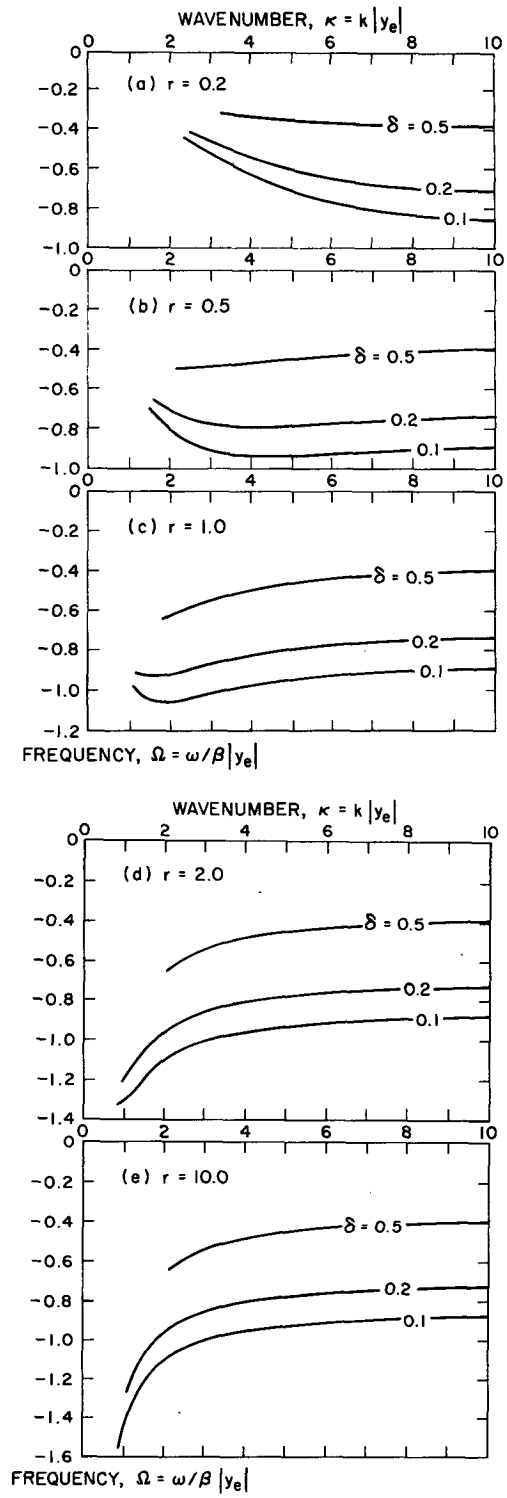

FIG. 3. The dispersion relation (4.7) for $y_e < 0$. The parameters r and δ are the same as in Fig. 2.

the case $y_e > 0$ and $\delta_1 = 1/\delta_0$ (shelf break in Northern Hemisphere and deep water to the south).

A few numerical examples of the period and phase speed of an equatorial shelf wave are given in Table 2 for the case in which the shelf break is located either 500 km north or 500 km south of the equator. We note that the wavelength 1300 km essentially corresponds to the long-wave cutoff at $K \approx 2.4$ shown in Fig. 3a. In contrast to the escarpment results shown in Table 1, we see that the westward propagating shelf waves ($y_e < 0$) travel only marginally faster than the eastward traveling waves ($y_e > 0$).

5. Trapped waves on a sloping beach

One of the main shortcomings of the discontinuous depth profile used in the previous two sections is that it permits only one mode of oscillation. The simplest smooth, continuous profile which will admit an infinity of modes is the uniformly sloping beach

$$H(y) = H_0 + \alpha y, \tag{5.1}$$

where $\alpha > 0$ (<0) corresponds to deep water to the north (south). The profile (5.1) has had a long history in the theory of coastally trapped waves at mid-latitudes (see LeBlond and Mysak, 1977). Therefore it is of considerable interest to determine the properties of the long-period waves that are trapped over a sloping beach that is located near the equator. The substitution of (5.1) into the amplitude equation (2.6) gives

$$(H_0 + \alpha y)\psi'' - \alpha\psi' - [(k^2 + k\beta/\omega)H_0 + \alpha k^2 y]\psi = 0. \tag{5.2}$$

For the sake of definiteness we first consider the case $\alpha > 0$ (deep water to the north), for which the domain of (5.2) is $-H_0/\alpha \leq y \leq \infty$. The transformation

$$y^* = y + H_0/\alpha \tag{5.3}$$

takes the above domain into $0 \leq y^* \leq \infty$. Next we introduce the dimensionless coordinate

$$\eta = ky^*, \tag{5.4}$$

which is positive since $k > 0$. In terms of the new independent variable η, Eq. (5.2) takes the form

$$\eta\psi_{\eta\eta} - \psi_\eta - (\eta + \lambda)\psi = 0, \; 0 \leq \eta \leq \infty, \tag{5.5}$$

where the eigenvalue λ is given by

$$\lambda = \beta H_0/\alpha\omega. \tag{5.6}$$

The boundary conditions (2.8) and (2.7b) become

$$\psi = 0 \quad \text{at} \quad \eta = 0 \tag{5.7}$$

and

$$\psi \to 0 \quad \text{as} \quad \eta \to \infty. \tag{5.8}$$

The system (5.5), (5.7) and (5.8) constitutes a two-point boundary value problem on the positive half-line with λ as the eigenvalue. Once the eigenvalues λ_n are known, the eigenfrequencies ω_n of the different modes are determined from (5.6). Since λ is independent of k, the eigenfrequencies will also be independent of k!

Eq. (5.5) can be transformed into a confluent hypergeometric equation, which then has to be solved subject to a modified form of the conditions (5.7), (5.8). However, a more direct approach involves solving the original system by means of the Laplace transform. If we apply the Laplace transform defined by

$$\bar{\psi}(s) = \int_0^\infty e^{-\eta s}\psi(\eta)d\eta \tag{5.9}$$

to (5.5) and invoke (5.7), we find that $\bar{\psi}(s)$ satisfies the first-order differential equation

$$\frac{d\bar{\psi}}{ds} = -\frac{3s + \lambda}{s^2 - 1}\bar{\psi}. \tag{5.10}$$

The general solution of (5.10) is

$$\bar{\psi}(s) = \frac{A_\lambda}{(s-1)^{(3+\lambda)/2}(s+1)^{(3-\lambda)/2}}, \tag{5.11}$$

where A_λ is an arbitrary constant. Hence $\psi(\eta)$ is given by

$$\psi(\eta) = \frac{1}{2\pi i}\int_{-i\infty+\gamma}^{i\infty+\gamma} \bar{\psi}(s)e^{\eta s}ds, \quad \gamma > 1, \tag{5.12}$$

where $\bar{\psi}(s)$ is the function defined in (5.11). For arbitrary values of λ, $\bar{\psi}(s)$ has branch points at $s = \pm 1$ and hence (5.12) will have a dominant behavior like e^η as $\eta \to \infty$, which violates the condition (5.8). However, this difficulty can be avoided if we set $(3 + \lambda)/2 = -n$, $n = 0, 1, 2, \ldots$, that is, take λ to have the discrete values

$$\lambda_n = -2n - 3, \quad n = 0, 1, 2, \ldots. \tag{5.13}$$

Thus, as there is now no singularity at $s = 1$ we can set $\gamma = 0$ and obtain the eigenfunctions by evaluating the contour integral

TABLE 2. The period and phase speed of an equatorial shelf wave on a flat shelf for three prescribed wavelengths. In all cases $\delta = H_2/H_1 = 0.1$ and $r = l/|y_e| = 0.2$, which are values of δ and r also used in Figs. 2 and 3. For $|y_e| = 500$ km, the value $r = 0.2$ corresponds to a shelf width of 100 km.

Wavelength (km)	Period (days)		Phase speed (km day^{-1})	
	$y_e = 500$ km,	$y_e = -500$ km	$y_e = 500$ km,	$y_e = -500$ km
500	9.8	8.2	51.0	60.0
1000	14.2	11.8	70.4	84.8
1300	17.7	14.2	73.5	91.6

$$\psi_n(\eta) = \frac{A_n}{2\pi i}\int_{-i\infty}^{i\infty} \frac{(s-1)^n}{(s+1)^{n+3}} e^{\eta s} ds, \qquad n = 0, 1, 2, \ldots$$

$$= \frac{A_n}{(n+2)!}\left\{\frac{d^{n+2}}{ds^{n+2}}[e^{\eta s}(s-1)^n]\right\}_{s=-1}. \quad (5.14)$$

On carrying out the differentiations in (5.14), we find that

$$\psi_n(\eta) = \frac{n!}{(n+2)!} A_n e^{-\eta}\eta^2 L_n^{(2)}(2\eta), \qquad n = 0, 2, \ldots, \quad (5.15)$$

where $L_n^{(2)}(z)$ is the generalized Laguerre polynomial of degree n; it is a solution of the special confluent hypergeometric equation (Abramowitz and Stegun, 1965, p. 509)

$$zw'' + (3-z)w' + nw = 0, \; n = 0, 1, \ldots. \quad (5.16)$$

The polynomials take the form

$$\left.\begin{aligned} L_0^{(2)}(z) &= 1 \\ L_1^{(2)}(z) &= 3 - z \\ L_2^{(2)}(z) &= 6 - 4z + z^2/2 \\ &\vdots \\ L_n^{(2)}(z) &= \sum_{m=0}^{n} \frac{1}{m!}\binom{n+2}{n-m}(-z)^m \end{aligned}\right\}. \quad (5.17)$$

Thus we see that the nth mode has n nodal lines parallel to the shoreline located $\eta = 0$. The polynomials (5.17) form a complete set on the interval $(0,\infty)$ and are orthogonal with respect to the weight function z^2e^{-z}. To obtain the eigenfunctions in terms of y, we simply put $\eta = k(y + H_0/\alpha)$ [see (5.3) and (5.4)] into the right side of (5.15).

Substituting (5.13) into (5.6), we find that the eigenfrequencies are given by

$$\omega_n = -\frac{H_0\beta}{\alpha(2n+3)}, \quad n = 0, 1, 2, \ldots, \quad (5.18)$$

where, we recall, $\alpha > 0$. The analogous result for trapped quasi-geostrophic nondivergent waves on a mid-latitude sloping beach is given by (Reid, 1958)

$$\omega_n = \frac{f}{2n+3}, \quad n = 0, 1, 2, \ldots, \quad (5.19)$$

where f is the (constant) Coriolis parameter.[4] The difference between these two formulas can be accounted for heuristically as follows. We first note that the equatorial and mid-latitude Rossby numbers are defined as $U/\beta L^2$ (Moore and Philander, 1977) and U/fL, respectively, where L is a horizontal length scale. Therefore to go from the latter to the former Rossby number we replace f by βL. Similarly, (5.18) can be obtained from (5.19) by replacing f in the latter by βL, where L is identified as $-H_0/\alpha$, the distance between the shoreline and the equator. If $H_0 < 0$ (>0), the shoreline is in the Northern (Southern) Hemisphere and, accordingly, Eq. (5.18) implies that the wave phase propagates with the shallow water to the right (left). Thus again the rule found in Sections 3 and 4 applies to the equatorial sloping beach. Eq. (5.19) also conforms to this rule if we recall that $f > 0$ (<0) in the Northern (Southern) Hemisphere. It is interesting to note that both (5.18) and (5.19) are independent of k and hence the group velocity in each case is zero: the waves propagate no energy. Another example of such an inert, long-period wave is the nondivergent, double Kelvin wave on the f-plane, whose dispersion relation is given in Eq. (3.4)′ (Rhines, 1967, 1969). Lastly, we observe that $\omega_n \equiv 0$ for the equatorial wave if $H_0 = 0$ (shoreline on the equator). This result can be interpreted as follows: In this case, the phase velocity is the average of the velocities for the cases $H_0 > 0$ and $H_0 < 0$ and hence is zero.

When $\alpha < 0$ (deep water to the south), we can again introduce the mapping (5.3). However, in place of η defined in (5.4), we use the variable $\eta' = -ky^*$. Proceeding as before, we now find that, for $\alpha < 0$,

$$\omega_n = \frac{H_0\beta}{\alpha(2n+3)}, \quad n = 0, 1, 2, \ldots, \quad (5.20)$$

but that the eigenfunctions $\psi_n(\eta')$ are also given by (5.15) with η replaced by η'. However, to get the eigenfunctions in terms of y, η' has to be replaced by $-k(y + H_0/\alpha)$. We note that (5.20) also concurs with the phase propagation rule. Consequently, (5.18) and (5.20) can be combined into the one relation valid for all α:

$$\omega_n = -\frac{H_0\beta}{|\alpha|(2n+3)}, \quad n = 0, 1, 2, \ldots. \quad (5.21)$$

[4] The formula given in (5.19) is obtained in the process of solving the mid-latitude amplitude equation (7.1) in which $\beta_0 = 0$, f = constant and $H = \alpha y$. If we take the formal nondivergent limit $g \to \infty$ (or $k \to \infty$) in Reid's (1958) dispersion relation [Eq. (33) in LeBlond and Mysak, 1977], which is obtained by solving an eigenvalue equation for the surface elevation, we obtain $\omega_n = f/(2n+1)$, $n = 0, 1, 2, \ldots$. Thus by starting the analysis from the nondivergent equations we automatically have eliminated one of the modes (the inertial mode $\omega = f$ in the case of Reid's quasi-geostrophic wave, and the mode $\omega = -H_0\beta/\alpha$ in the case of the long-period equatorial sloping beach wave discussed here). Finally, we note that while the eigenfrequencies for the long-period equatorial and mid-latitude sloping beach waves are quite different, the eigenfunctions ψ_n in both cases take the form (5.15).

The period T_0 of the gravest mode trapped on a sloping beach whose coastline is either 500 km north or 500 km south of the equator is 19.1 days (see Table 3). The higher modes have longer periods since $T_n \propto 2n + 3$, where $T_n = 2\pi/|\omega_n|$.

6. Trapped waves on an exponential depth profile

As our final example, we seek trapped wave solutions for the Ball (1967) depth profile given by

$$H = H_1[1 - e^{-a(y-y_c)}], \quad y_c \leq y \leq \infty, \tag{6.1}$$

where $a > 0$ (deep water to the north). Close to the shoreline $[a(y - y_c) \ll 1]$, the profile (6.1) reduces to the sloping beach profile (5.1), i.e.,

$$H \approx -H_1 a y_c + H_1 a y \equiv H_0 + \alpha y. \tag{6.2}$$

However, as $y \to \infty$ the depth increases monotonically to a constant (H_1). If (6.1) is written in the form (for $y_c > 0$)

$$H = H_1(1 - e^{-\gamma(Y-1)}], \quad 1 \leq Y \leq \infty, \tag{6.3}$$

where $\gamma = ay_c$ and $Y = y/y_c$, we notice that the magnitude of the parameter γ determines how quickly the depth increases away from the shoreline. For small (large) γ, (6.3) implies that the depth increases very slowly (quickly) as Y increases away from unity. We shall call γ the growth rate of the depth profile. Finally, we observe that if $a < 0$, then (6.1) can also be used to describe the situation with deep water to the south provided we redefine the domain of $H(y)$ as $-\infty \leq y \leq y_c$.

The substitution of (6.1) into (2.6) yields

$$[1 - e^{-a(y-y_c)}]\psi'' - ae^{-a(y-y_c)}\psi' - \{[1 - e^{-a(y-y_c)}]k^2 + (k\beta/\omega)[1 - (1 + ay)e^{-a(y-y_c)}]\}\psi = 0. \tag{6.4}$$

The appropriate boundary conditions are

$$\psi = 0 \quad \text{at} \quad y = y_c, \tag{6.5}$$

and

$$\psi \to 0 \quad \text{as} \quad y \to \infty \quad (a > 0), \tag{6.6a}$$

or

$$\psi \to 0 \quad \text{as} \quad y \to -\infty \quad (a < 0). \tag{6.6b}$$

It is now convenient to introduce the new independent variable z defined by

TABLE 3. The period and phase speed of the gravest mode ($n = 0$) trapped wave on a sloping beach for two prescribed wavelengths. According to (5.21), the period of this mode, for either westward or eastward propagation, is $T_0 = 6\pi/\beta L$, where $L = |H_0|/|L|$ is the distance between the coastline and the equator. In computing T_0 below we have set $L = 500$ km.

Wavelength (km)	Period (days)	Phase speed (km day^{-1})
1000	19.1	52.4
3000	19.1	157

$$z = e^{-a(y-y_c)} - 1. \tag{6.7}$$

Under the transformation (6.7), the domains $y_c \leq y \leq \infty$ $(a > 0)$ and $-\infty \leq y \leq y_c$ $(a < 0)$ are both mapped into the finite interval $-1 \leq z \leq 0$. In terms of z, Eqs. (6.4)–(6.6) become, for both $a > 0$ and $a < 0$,

$$z(z + 1)^2 \frac{d^2\psi}{dz^2} - (z + 1)\frac{d\psi}{dz} + [-(\hat{k}^2 + \hat{k}/\hat{\omega})z - (\hat{k}\gamma/\hat{\omega})(z + 1) + (\hat{k}/\hat{\omega})(z + 1)\log(z + 1)]\psi = 0, \quad -1 \leq z \leq 0, \tag{6.8}$$

$$\psi = 0 \quad \text{at} \quad z = 0, \tag{6.9a}$$

$$\psi = 0 \quad \text{at} \quad z = -1, \tag{6.9b}$$

where $\gamma = ay_c$, $\hat{k} = k/|a| > 0$ and $\hat{\omega} = \omega|a|/\beta$. Because of the presence of both algebraic and transcendental coefficients in (6.8), there are no solutions of this equation in terms of known special functions. By way of contrast, the corresponding equation for waves on a mid-latitude exponential profile on an f-plane does not contain the logarithmic term and consequently has solutions in terms of hypergeometric functions (Ball, 1967).

We observe that the Eq. (6.8) has a regular singular point at $z = 0$ and an irregular singular point at $z = -1$. Therefore we can use the method of Frobenius to find a series solution of (6.8) in powers of z. First, however, it is necessary to expand the term $(z + 1)\log(z + 1)$ in (6.8) in a Taylor series about $z = 0$. The resulting equation we thus wish to solve is

$$z(z^2 + 2z + 1)\frac{d^2\psi}{dz^2} - (z + 1)\frac{d\psi}{dz} + [-\gamma\theta + (\hat{k}^2 + \gamma\theta)z + \theta\sum_{n=1}^{\infty} b_{n+1}z^{n+1}]\psi = 0, \quad -1 \leq z \leq 0, \tag{6.10}$$

subject to the boundary conditions (6.9). In (6.10) θ is the inverse of the nondimensional phase speed, *viz.*,

$$\theta = \hat{k}/\hat{\omega}, \tag{6.11}$$

and the coefficient b_{n+1} is defined by

$$b_q = \frac{(-1)^q(q - 2)!}{q!}, \quad q = 2, 3, \ldots. \tag{6.12}$$

We now seek a solution of (6.10) of the form

$$\psi = \sum_{m=0}^{\infty} a_m z^{m+p}, \quad a_0 \neq 0. \tag{6.13}$$

Substitution of (6.13) into (6.10) yields the indicial equation

$$p(p - 2) = 0, \tag{6.14}$$

with solutions $p_1 = 2$ and $p_2 = 0$. It is clear that (6.13) will satisfy (6.9a) only if we choose $p_1 = 2$. (The second root $p_2 = 0$ leads to a second linearly independent solution which is logarithmically singular at $z = 0$.) For the root $p_1 = 2$, the recurrence relation reduces to

$$(r + 3)(r+ 5)a_{r+3} + [(r + 4)(2r + 5) - \gamma\theta]a_{r+2} + [(r + 2)(r + 3) - \hat{k}^2 - \gamma\theta]a_{r+1} + \theta d_{r+2} = 0, \quad r = -2, -1, 0, 1, 2, \ldots, \quad (6.15)$$

where

$$\left.\begin{aligned} a_n &\equiv 0 \quad \text{for} \quad n \leqslant -1 \\ d_n &= \sum_{j=0}^{n-2} b_{n-j}a_j, \quad n = 2, 3, \ldots \\ &\equiv 0 \quad \text{for} \quad n \leqslant 1 \end{aligned}\right\}.$$

The dispersion relation for each mode is determined by applying the condition (6.9b) to the solution (6.13), *viz.*,

$$0 = \sum_{m=0}^{\infty} a_m(-1)^m. \quad (6.16)$$

Since the series (6.16) converges rapidly, we can truncate it after N terms and hence determine good approximations to the dispersion relations $\hat{\omega}_n(\hat{k})$ of the first few modes ($n = 1,2, \ldots, n_N \ll N$). The larger N is, of course, the better the approximations become. Using (6.15) repeatedly we can express each coefficient in the truncated series obtained from (6.16) in the form

$$a_m = a_0 F_m(\theta,\hat{k},\gamma), \quad m = 1,2, \ldots, N,$$

where F_m is a polynomial in θ of degree m. Thus after some rearrangement, the truncated form of (6.16) can be written

$$0 = A_0 + A_1\theta + A_2\theta^2 + \ldots + A_N\theta^N, \quad (6.17)$$

where $A_m = A_m(\hat{k},\gamma)$. We now set $\gamma = \gamma_0$, a fixed growth rate for a given topography [see (6.3)], and solve (6.17) for the roots θ_n, $n = 1, \ldots, N$, as a function of wavenumber $\hat{k}$ for $0 < \hat{k} < \hat{k}_0$. Then from (6.11) we can determine the approximations to $\hat{\omega}_n(\hat{k}; \gamma_0)$, the dispersion relation of the nth mode corresponding to the preassigned decay rate γ_0. The results for the first three modes ($n = 1,2,3$), ordered according to decreasing values of $\hat{\omega}_n$ for a fixed $\hat{k}$, are shown in Fig. 4 ($\gamma > 0$) and Fig. 5 ($\gamma < 0$). To compute these curves we used $N = 20$.

Examination of Fig. 4 reveals that for each mode $\hat{\omega}_n$ tends to a constant as $\hat{k}$ increases, i.e., at large wavenumbers $\hat{\omega}_n$ is independent of wavenumber. This is in qualitative agreement with the formula for ω_n for the sloping beach, which is strictly independent of wavenumber, since for large $\hat{k}$ we expect the waves on profile (6.1) to be trapped *near* the shoreline where the exponential profile is approximately

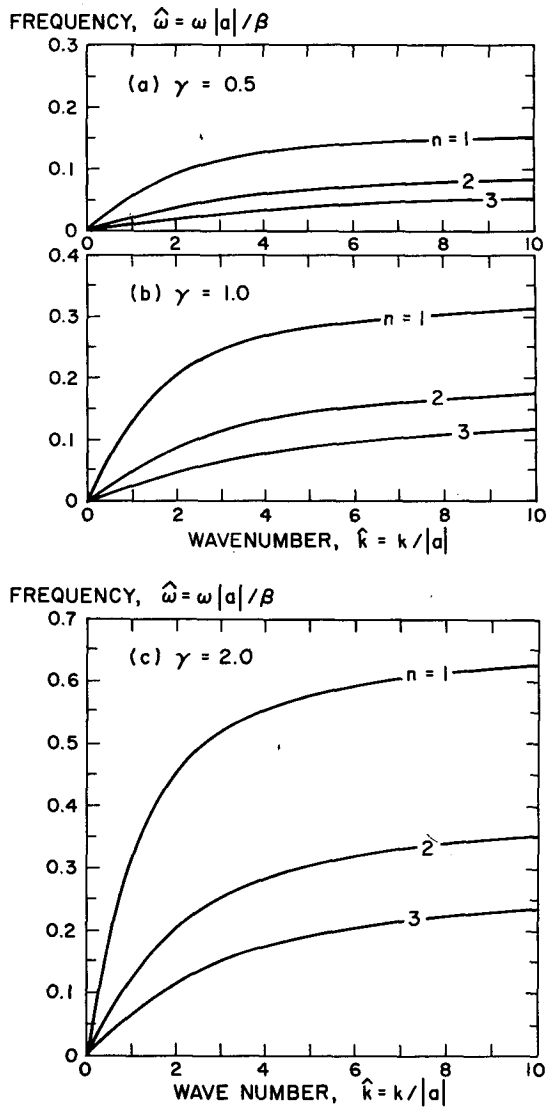

FIG. 4. The dispersion curves of the first three modes (n = 1,2,3) for the depth profile (6.1) for different values of the growth rate $\gamma = ay_c > 0$. Note that $\gamma > 0$ when a, $y_c > 0$ (deep water to the north, shoreline in Northern Hemisphere) or a, $y_c < 0$ (deep water to the south, shoreline in Southern Hemisphere).

linear. Note that this "agreement" is especially good for $\gamma = 0.5$ (Fig. 4a), where $\hat{\omega}_n \approx$ constant for $\hat{k} \gtrsim 7$. A second fact to note from Fig. 4 is that for a fixed mode at a given wavenumber, $\hat{\omega}_n$ increases with γ, or equivalently, with the bottom slope, since $dH/dy \propto \gamma$ [see (6.3)]. This property is also true for topographic planetary waves at mid-latitudes. Finally we note that the phase and energy always propagate in the same direction (eastward), and that the direction of phase propagation is in accordance with our general rule [shallow water to the right (left) in the Northern (Southern) Hemisphere]. These general results are qualitatively similar to those for long-period waves trapped on this profile at mid-latitudes (Ball, 1967).

We first note from Fig. 5 that for a fixed γ, $\hat{\omega}_n$ again tends to a constant as $\hat{k} \to \infty$, as in Fig. 4, with the constant being the negative of the corresponding constant in Fig. 4. This is to say, for a fixed $|\gamma|$ the dispersion curves are nearly symmetrical about the $\hat{k}$ axis for large $\hat{k}$, which is in agreement with the symmetry of (5.21) with respect to $\alpha > 0$ and $\alpha < 0$. Second, we observe that the phase now propagates westward (in accordance with our general rule), but that the group velocity c_g changes direction with increasing $\hat{k}$. For "small" γ (Fig. 5a), c_g and c (the phase velocity) are in the same direction for small $\hat{k}$, and in opposite directions at large $\hat{k}$. (This also occurred for two values of r in the flat shelf model—see Figs. 3b and 3c.) However, it is interesting to note that for "large" γ (Fig. 5c), $c_g = 0$ at *two* values of $\hat{k}$, so that c_g and c are in the same direction at small and large $\hat{k}$, but in opposite directions at intermediate $\hat{k}$! This result appears to be unique to the equator; the author is unaware of any topographies for which mid-latitude shelf waves have *two* zero group velocities. Finally, we note that, unlike the flat shelf case, there is *no* long-wave cutoff for trapped waves. This is because for $\gamma < 0$ the bottom slope occurs on *both* sides of the equator and is always able to provide a restoring force to counteract that due to β.

A few numerical examples of the period and phase speed of the gravest mode ($n = 1$) trapped wave on the exponential profile (6.1) are given in Table 4. We again note the same numerical asymmetry in the phase speeds as found earlier for the escarpment and flat shelf phase speeds: the westward traveling waves ($y_c < 0$) travel faster than the eastward traveling waves ($y_c > 0$).

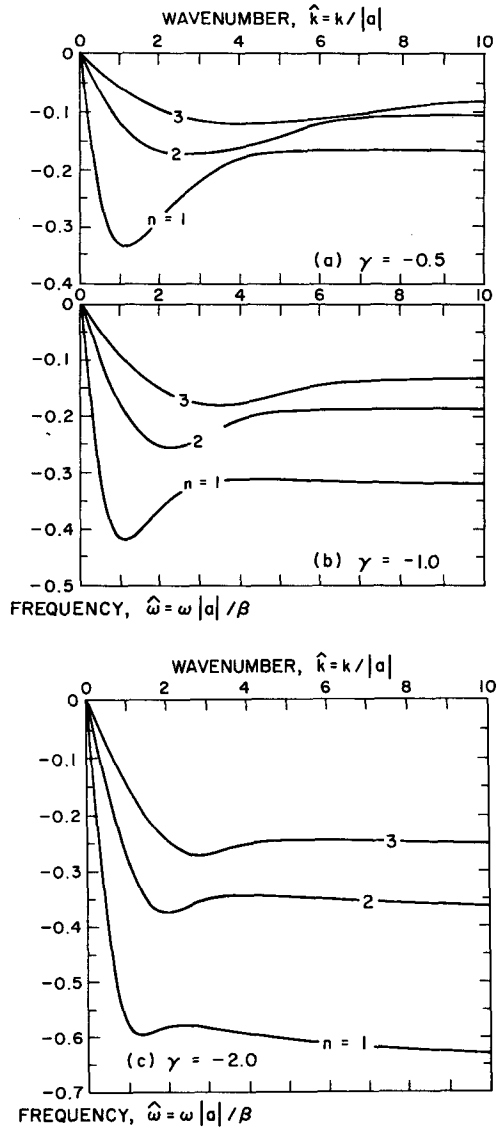

FIG. 5. The dispersion curves of modes $n = 1,2,3$ for the depth profile (6.1) for $\gamma = ay_c < 0$, which occurs when $a > 0$, $y_c < 0$ (deep water to the north, shoreline in Southern Hemisphere) or $a < 0$, $y_c > 0$ (deep water to the south, shoreline in Northern Hemisphere).

7. Qualitative results

In the last four sections we presented solutions for trapped equatorial waves over a variety of depth profiles. In this section we first give a WKB-type argument[5] which shows that trapped waves will always exist near the equator over a monotonic, slowly varying depth profile. We then derive a simple criterion which can be used to determine the sign of the phase speed for any prescribed depth profile. Finally, we prove that any two distinct amplitude eigenfunctions corresponding to two distinct eigenfrequencies are orthogonal with respect to the weight function $[y/H(y)]'$.

The linearized vorticity equation analogous to the amplitude equation (2.6) for the case of mid-latitude zonally propagating waves takes the form

$$\psi'' - \frac{H'}{H}\psi' - \left[k^2 + \frac{k}{\omega}\left(\beta_0 - \frac{fH'}{H}\right)\right]\psi(y) = 0, \quad (7.1)$$

where $f = 2\Omega_E \sin\phi_0 + (2\Omega_E \cos\phi_0/R)y \equiv f_0 + \beta_0 y$, ϕ_0 being the mean latitude. Provided $\psi' \sim k\psi$, it follows that the first topographic term in (7.1) is much smaller than the second topographic term for long-period waves ($f/\omega \gg 1$). Therefore, the term $-H'\psi'/H$ can be neglected; this is Rhines' (1969) so-called "first approximation". Second, since the term proportional to β_0 accounts for the latitudinal variation in f, we can replace f by its mean value f_0 in the second topographic term [Rhines' (1969) "second approximation"]. Finally, we suppose that H is sufficiently slowly varying so that the slope

[5] I am indebted to Dr. F. P. Bretherton for suggesting this argument.

TABLE 4. The period and phase speed of the gravest mode ($n = 1$) trapped wave on the exponential profile (6.1) in which $a^{-1} = 500$ km and $y_c = \pm 500$ km. For these values, $\gamma = 1$ ($y_c = 500$ km) or $\gamma = -1$ ($y_c = -500$ km).

Wavelength (km)	Period (days)		Phase speed (km day^{-1})	
	$y_c = 500$ km,	$y_c = -500$ km	$y_c = 500$ km,	$y_c = -500$ km
1000	25.5	20.2	39.2	49.5
3000	45.5	15.4	65.9	195

$H' = \alpha$ can be treated as constant. Under these approximations, we can thus replace (7.1) by

$$\psi'' - \left[k^2 + \frac{k}{\omega}\left(\beta_0 - \frac{\alpha f_0}{H(y)}\right)\right]\psi = 0, \qquad (7.2)$$

in which α and f_0 are constants and $H(y)$ is a slowly varying function of y. Under the latter hypothesis, (7.2) will have a solution of the form

$$\psi \propto e^{il(y)y}, \qquad (7.3)$$

where $l(y)$ is a slowly varying north-south wavenumber, provided

$$\omega = k\left(\frac{\alpha f_0}{H(y)} - \beta_0\right)\Big/[k^2 + l^2(y)]. \qquad (7.4)$$

The dispersion relation (7.4), which is valid near a fixed latitude ϕ_0, can now be used to show that over a monotonic depth profile which straddles the equator and for which $[\alpha f_0/H(y)] - \beta_0 > 0$ when $\alpha f_0 > 0$, the solution far from the equator on one side must be of a decaying nature and, far on the other side, oscillatory. For definiteness, let us suppose that $H(y)$ increases ($\uparrow$) as y increases ($\uparrow$) and hence $\alpha > 0$ (deepening water to the north). Then starting from a fixed latitude ϕ_0 in the Northern Hemisphere, where $f_0 > 0$, the numerator in (7.4) decreases ($\downarrow$) as $y\uparrow$. Thus for the wave frequency ω to remain constant, $k^2 + l^2(y)$ must decrease as $y\uparrow$. But for sufficiently large y (and hence H), we eventually reach a latitude where $l^2(y)$ must become negative so that the denominator can continue decreasing as $y\uparrow$. This is to say, the north-south wavenumber eventually becomes pure imaginary and (7.3) therefore implies a decaying behavior sufficiently far to the north of the equator. Starting from a fixed latitude $-\phi_0$ in the Southern Hemisphere, where $f_0 < 0$, the numerator in (7.4) becomes more negative as $y\downarrow$ (the shoreline is approached). Therefore the frequency in (7.4) remains constant only if $l^2(y)\uparrow$. This is to say, the amplitude is oscillatory far to the south of the equator.

In a similar manner it is easy to show that if $H(y)\uparrow$ as $y\downarrow$ (deepening water to the south), there must now be a decaying behavior far to the south of the equator and an oscillatory behavior far to the north. We must emphasize that these results are strictly qualitative in nature. The argument we have presented only establishes the existence of a trapped wave near the equator; it provides no details about the precise structure of the solution near the equator and it does not predict the direction of propagation near the equator.

We note here that the WKB argument given above for the existence of trapped waves near the equator is critically dependent on treating f as locally constant and on having the depth varying monotonically across the equator. For the usual equatorially trapped waves in an ocean of constant depth, it is the rapidly varying f near the equator that is important, a feature which gives rise to two "turning latitudes" symmetrically located on either side of the equator. Outside the band formed by these two turning latitudes, the amplitude equation for equatorially trapped waves has decaying solutions, and inside this band, oscillatory solutions.

We now derive a simple criterion which can be used to determine the direction of phase propagation over any prescribed depth profile. If (2.6) is multiplied by ψ and the resulting equation integrated over the domain D ($-\infty \leq y \leq \infty$ or $y_c \leq y \leq \infty$ say), we obtain

$$\left.\frac{\psi\psi'}{H}\right|_D - \int_D \frac{\psi'^2}{H}\,dy - k^2\int_D \frac{\psi^2}{H}\,dy - \frac{\beta}{c}\int_D \left(\frac{y}{H}\right)'\psi^2 dy = 0, \qquad (7.5)$$

where $c = \omega/k$ and $c < 0$ (>0) corresponds to westward (eastward) phase propagation. Since $\psi'/H \propto u$ and $\psi = 0$ at the boundaries, the first term vanishes provided u is bounded, which will be true for all continuous depth profiles. Thus (7.5) gives the following formula for c:

$$c = \frac{-\beta\int_0 \psi^2(y/H)'dy}{\int_D (1/H)(\psi'^2 + k^2\psi^2)dy}. \qquad (7.6)$$

Since $\beta > 0$ and the denominator of (7.6) is positive, it follows from (7.6) that $c < 0$ (>0) according to whether y/H, which is proportional to the equilibrium potential vorticity $\beta y/H(y)$, is a monotone increasing (decreasing) function of y.

The above theorem succinctly summarizes the results concerning the direction of phase propagation we found for specific depth profiles. For example, in the sloping beach solution we found that $c < 0$ for the case $H_0 > 0$ and $\alpha > 0$ (see Section 5). The result $c < 0$ now directly follows from the theorem since for this profile

$$\frac{y}{H(y)} = \frac{1}{\alpha + H_0/y}\uparrow \quad \text{as} \quad y\uparrow.$$

Finally, let us suppose that ψ_n, $\omega_n(k)$ and ψ_m, $\omega_m(k)$ are two distinct amplitude eigenfunctions and eigenfrequencies that are solutions of (2.6) and the homogeneous boundary conditions [(2.7a) or (2.7b), (2.8)]. In the usual manner, it readily follows from the two equations for ψ_n and ψ_m that

$$\frac{k\beta(\omega_m - \omega_n)}{\omega_m\omega_n}\int_D \left(\frac{y}{H}\right)' \psi_m\psi_n dy = 0. \quad (7.7)$$

Thus provided y/H is either strictly monotone increasing or monotone decreasing (in which case the phase speeds have a fixed sign!), Eq. (7.7) implies that the eigenfunctions are orthogonal on D with respect to the weight function $(y/H)'$.

8. Summary and discussion

The propagation of long-period, barotropic nondivergent waves parallel to the equator over a variety of depth profiles $H(y)$ has been investigated theoretically. It was found that the waves are always trapped near the equator, a result which was also established heuristically for any monotonic profile $H(y)$. The solutions obtained were particularly simple for $H(y)$ corresponding to 1) a single-step escarpment, 2) a flat shelf and 3) a uniformly sloping beach. In case 3 for example, the frequency of the nth mode ($n = 0,1,2, \ldots$) is given by $\omega_n = -\beta H_0/|\alpha|(2n + 3)$ for all zonal wavenumbers $k > 0$, where α is the bottom slope and $y = -H_0/\alpha$ is the position of the shoreline (where $H = 0$). Finally, it was proved that the wave phase propagates westward or eastward according to whether the equilibrium potential vorticity $\beta y/H(y)$ is a monotone increasing or decreasing function and that the amplitude eigenfunctions are orthogonal with respect to the weight function $(y/H)'$.

In the light of the above elementary theory of equatorial topographic waves, it is now natural to ask where these waves may be observed in the ocean. First, it is conceivable that the equatorial double Kelvin wave could propagate along the Colon-Ecuador Ridge (which extends eastward of the Galapagos Islands) or along the equatorial part of the mid-Atlantic Ridge. Second, east-west oriented equatorial continental shelf/slope regions occur in the Gulf of Guinea, West Africa, off the north coast of New Guinea and off the north and south coasts of northeast Celebes, and therefore equatorial shelf waves may exist in these regions. Indeed, Houghton and Beer (1976) found that in 1974 the sea surface temperature along the coast of Ghana (which runs approximately east-west on the north side of the Gulf of Guinea) exhibited periodic variations at a frequency of 0.07 cycles per day (cpd) which propagated westward along the coast. The average speed of this signal was computed to be 55 km day^{-1}. A similar westward propagating wave of this frequency was also observed by J. Picaut and J. M. Verstraete (personal communication) along the more extensive Ghana-Ivory coast. They estimated the average speed to be 47 km day^{-1}. Houghton and Beer (1976) suggested that this wave is most likely an internal Kelvin wave, whereas Picaut and Verstraete suggested that the observed oscillation may be tidal in origin, arising out of a nonlinear interaction between the M_2 and S_2 tides in the northeast corner of the Gulf of Guinea. It is suggested here that this wave may also be interpreted as an equatorial shelf wave. From the dispersion relation (4.6) for a flat shelf with deep water to the south, we obtain a phase velocity directed westward of 91.6 km day^{-1}, which corresponds to a period and wavelength of 14.2 days (0.07 cpd) and 1300 km, respectively, and to the topographic values $l = 100$ km, $y_e = 500$ km and $H_2/H_1 = 10$. These topographic values approximately describe the situation off the Ghana coast. Although this theoretical speed is about 65% higher than the observed speed, it is sufficiently close to warrant further observations and development of the theory to see whether equatorial shelf waves do in fact exist in this region.

With regard to further development of the theory, we again emphasize that the most idealized model for equatorial topographic waves has been used in this paper. Natural extensions of the theory, analogous to those that have been carried out for mid-latitude double Kelvin and shelf waves, include studying the effects of a finite-width sloping shelf (Mysak, 1968),[6] free-surface divergence (Reid, 1958; Longuet-Higgins, 1968), a laterally sheared mean flow (Niiler and Mysak, 1971; Tareyev, 1971; Brooks and Mooers, 1977), and deep sea (Mysak, 1967) or nearshore (Kajiura, 1974; Wang and Mooers, 1976) stratification. A number of these extensions of the theory are now being investigated, and the results will be reported in a future paper.

In closing, we now raise the following interesting questions, mentioned briefly in the Introduction: will equatorial topographic waves play an important role in the time-dependent response of the tropical ocean? It is conjectured that they will since the length and time scales of such phenomena as the Somali Current formation and El Niño (which occur in regions of variable topography) are of the same order as the typical wavelength and period of the waves discussed here, namely, O(1000 km) and O(weeks). However, in connection with the Somali current, it is noted that off the east coast of Africa the shelf/slope contours are inclined at approximately 45° to the equator. The modification of the theory discussed here to handle such nonzonal contours is likely to be a challenging problem.

[6] The references quoted hereafter treat these various effects for the case of mid-latitude waves.

Acknowledgments. This paper was written while the author was visiting the National Center for Atmospheric Research (Oceanography Project) during the period February–August 1977. The author is indebted to Mrs. Julianna Chow for plotting the curves shown in Figs. 2–5, to Ms. Karla Nolan for typing the manuscript and to Dr. P. R. Gent for criticizing a first draft of this paper.

REFERENCES

Abramowitz, M., and I. A. Stegun, 1965: *Handbook of Mathematical Functions*. Dover, 1046 pp.

Anderson, D. L. T., and P. B. Rowlands, 1976: The Somali current response of the southwest monsoon: The relative importance of local and remote forcing. *J. Mar. Res.*, **34,** 395–417.

Ball, F. K., 1967: Edge waves in an ocean of finite depth. *Deep-Sea Res.*, **14,** 79–88.

Brooks, D. A., and C. N. K. Mooers, 1977: Free, stable continental shelf waves in a sheared, barotropic boundary current. *J. Phys. Oceanogr.* **7,** 380–388.

Cox, M. D., 1976: Equatorially trapped waves and the generation of the Somali current. *Deep-Sea Res.*, **23,** 1139–1152.

Houghton, R. W., and T. Beer, 1976: Wave propagation during the Ghana upwelling. *J. Geophys. Res.*, **81,** 4423–4429.

Kajiura, K., 1974: Effect of stratification on long period trapped waves on the shelf. *J. Oceanogr. Soc. Japan*, **30,** 271–281.

Larsen, J. C., 1969: Long waves along a single-step topography in a semi-infinite uniformly rotating ocean. *J. Mar. Res.*, **27,** 1–6.

LeBlond, P. H., and L. A. Mysak, 1977: Trapped coastal waves and their role in shelf dynamics. *The Sea*, Vol. 6, E. D. Goldberg, I. N. McCave, J. J. O'Brien and J. H. Steele, Eds., Wiley-Interscience, 459–495.

——, and ——, 1978: *Waves in the Ocean*. Elsevier, 602 pp.

Longuet-Higgins, M. S., 1968: On the trapping of waves along a discontinuity of depth in a rotating ocean. *J. Fluid Mech.*, **31,** 417–434.

Moore, D. W., and S. G. H. Philander, 1977: Modeling of the tropical oceanic circulation. *The Sea*, Vol. 6., E. D. Goldberg, I. N. McCave, J. J. O'Brien and J. H. Steele, Eds., Wiley-Interscience, 319–361.

Mysak, L. A., 1967: On the theory of continental shelf waves. *J. Mar. Res.*, **25,** 205–227.

——, 1968: Edgewaves on a gently sloping continental shelf of finite width. *J. Mar. Res.*, **26,** 24–33.

Niiler, P. P. and L. A. Mysak, 1971: Barotropic waves along an eastern continental shelf. *Geophys. Fluid Dyn.*, **2,** 273–288.

Reid, R. O., 1958: Effects of Coriolis force on edge waves. (I) Investigation of normal modes. *J. Mar. Res.*, **16,** 109–144.

Rhines, P. B., 1967: The influence of bottom topography on long-period waves in the ocean. Ph.D. thesis, University of Cambridge.

——, 1969: Slow oscillations in an ocean of varying depth. Part I. Abrupt topography. *J. Fluid Mech.*, **37,** 161–189.

——, 1977: The dynamics of unsteady currents. *The Sea*, E. D. Goldberg, I. N. McCave, J. J. O'Brien and J. H. Steele, Eds., Vol. 6, Wiley-Interscience, pp. 189–318.

Tareyev, B. A., 1971: Gradient-vorticity waves on the continental shelf. *Izv. Akad. Nauk S.S.S.R. Fiz. Atmos. Okean.*, **7,** 431–436.

Wang, D.-P., and C. N. K. Mooers, 1976: Coastal-trapped waves in a continuously stratified ocean. *J. Phys. Oceanogr.*, **6,** 853–863.